

Optimal Perfusion Rate Determined for *In Situ* Intestinal Absorption Studies in Rats

PAUL M. SAVINA, A. E. STAUBUS^{*}, T. S. GAGINELLA, and D. F. SMITH

Received June 9, 1980, from the College of Pharmacy, Ohio State University, Columbus, OH 43201.

Accepted for publication August 13, 1980.

Abstract □ Iopanoic acid was used as a model compound to study the effects of the intestinal perfusion rate on the mean absorption clearance. Absorption of iopanoic acid followed first-order kinetics, with a first-order absorption rate constant (k_a) linearly dependent on the dry intestinal weight. An absorption clearance-time plot revealed three phases. Phase I represented an equilibration phase, Phase II was a uniform phase, and Phase III was a physiological deterioration of the animal under prolonged anesthesia. The variability in the observations during Phase II of the absorptive clearance-time profiles was assessed statistically, and the minimum occurred at 9.9 $\mu\text{l}/\text{sec}$ (0.594 ml/min). The relation between the coefficient of variance (CV) and the perfusion rate is given by $CV = (-5.52 \times 10^{-5})Q^3 + (2.78 \times 10^{-3})Q^2 - (3.87 \times 10^{-2})Q + 0.243$, where Q is the perfusion rate through the intestinal lumen. These studies demonstrate that an optimal flow rate exists for minimizing the variability in *in situ* absorption studies. The dependency of the absorption clearance on the intestinal perfusion rate appears to conform to the convective diffusion model.

Keyphrases □ Iopanoic acid—absorption from *in situ* rat small intestine, optimal perfusion rate determined □ Absorption, GI—iopanoic acid from *in situ* rat small intestine, optimal perfusion rate determined □ Models, pharmacokinetic—convective diffusion model, relationship between intestinal absorption clearance and intestinal perfusion rate, rats □ Perfusion rate—optimum, *in situ* intestinal absorption studies, rats

Drug absorption studies have utilized animal models and employed both *in vitro* and *in vivo* techniques. The clinical ramification of these studies is the delineation of the factors influencing drug absorption so as to maximize drug therapy from the standpoint of drug dosing, efficacy, and safety.

Results from *in vivo* studies often lack reproducibility. This problem may be due to a lack of attention on experimental design or the physiological conditions of the animal preparation (1). Factors that influence both solute absorption and transmucosal fluid movement include the constituents of the perfusates (1), pH (2–8), and bile salts (9–11). The flow rate through the intestine also significantly affects the absorption rate. The flow rate influenced the calcium absorption rate in dogs (12), and the *in vivo* perfusion method was used to determine the effect of flow rate on glucose absorption in rats (13). In another study (14), the perfusion load could predict glucose absorption in humans. Other studies (3, 4) investigated the effects of flow rates and other luminal factors influencing vitamins A₁ and K₁ absorption. In addition, the possible mechanisms by which changes in flow rate might affect drug absorption were studied (15).

Although each of these studies led to recommendations for the optimal experimental design for drug absorption studies, virtually no work has been reported on the effects of flow rates on the variability of absorption. Maintaining the variability at a minimum is important for valid comparisons between agents that may alter normal absorption. This study was designed to determine an optimal flow rate

at which variability in the mean absorption clearance of a model compound, iopanoic acid, could be minimized during *in situ* experiments.

EXPERIMENTAL

All chemicals were analytical reagent grade and were used as received. A modified Krebs buffer constituted the working isosmotic buffer, in which the iopanoic acid perfusion solution was prepared, and was composed of 25 mM NaHCO₃, 1.2 mM KH₂PO₄, 1.2 mM MgSO₄, 4.7 mM KCl, and 118.4 mM NaCl. The iopanoic acid perfusion solution was prepared by stirring excess iopanoic acid¹ with 1 liter of the buffer and filtering through a büchner funnel. The filtrate concentration of iopanoic acid was adjusted to 1.8 $\mu\text{moles}/\text{ml}$, and the resultant pH was 7.8 as measured on a pH meter².

Male albino Sprague-Dawley rats³, 200–300 g, were maintained in fully accredited animal care facilities⁴ on a 12-hr light cycle at 72 °F (11.1 °C) and 50% humidity for at least 1 week prior to use. The animals received food⁵ and water *ad libitum* but were fasted 12–16 hr before each experiment. Longer fasting times were not used to avoid possible deviations in absorption (16).

The surgical procedure was similar to that described by Schanker *et al.* (6). Anesthesia was induced by injection of urethan (1.5 mg/kg ip). A midventral abdominal incision extending 5–6 cm posteriorly to the pectoris minor was made, and the small intestine was exposed. The jejunum was located, and a small incision was made 6–8 cm below the ligament of Trietz. Care was taken not to cut through the segment completely. A similar incision was made 30 cm aboral to the first. The segment then was gently flushed with 30–40 ml of modified Krebs buffer until the effluent was clear and the segment was free of waste and debris. The flushing process was slow so as not overly to expand the intestine and cause damage due to high hydrostatic pressure.

The ends of the segment were cannulated with the needle adaptor end of a sterilized Travenol extension set and secured with encircling 00 surgical silk sutures fitted through the mesentery proper, between two branches of the superior mesenteric vein. The free end of the extension set cannulating the upper portion of the segment was attached to a Lambda infusion pump⁶, while the free end of the extension set cannulating the distal portion of the segment extended along the ventral surface of the rat into a 10-ml graduated cylinder. The intestinal segment then was placed within the abdominal cavity carefully to avoid crimping and kinking of the segment, which would lead to subsequent obstruction. The body temperature of the animal was maintained at 37° by a heating lamp and a constant-temperature device⁷ regulated by a thermister probe placed within the abdominal cavity. The abdominal incision, as well as any exposed intestine, then was covered with gauze sponges moistened with warmed buffer and changed throughout the study to ensure a clean moist cover.

The cannulated jejunal segments ranged from 20 to 30 cm in length and were perfused with iopanoic acid at one of the following flow rates: 2.1 $\mu\text{l}/\text{sec}$ (0.126 ml/min), 3.1 $\mu\text{l}/\text{sec}$ (0.186 ml/min), 4.2 $\mu\text{l}/\text{sec}$ (0.252 ml/min), 8.3 $\mu\text{l}/\text{sec}$ (0.498 ml/min), 12.5 $\mu\text{l}/\text{sec}$ (0.75 ml/min), 16.7 $\mu\text{l}/\text{sec}$ (1.002 ml/min), and 20.5 $\mu\text{l}/\text{sec}$ (1.23 ml/min) for 240–300 min. Drainage from the segment to the collecting cylinder was achieved by gravity. Samples were taken every 30 min for the perfusion rate of 2.1 $\mu\text{l}/\text{sec}$ and

¹ Telepaque, Sterling-Winthrop, Rensselaer, N.Y.

² Model 12, Corning Glass Works, Corning, N.Y.

³ Laboratory Supply Co., Indianapolis, Ind.

⁴ American Association for the Accreditation of Laboratory Animal Care.

⁵ Purina Rodent Laboratory Chow 5001.

⁶ Model 1301, Harvard Apparatus Co., Millis, Mass.

⁷ Thermistemp, model 74, Yellow Springs Instrument Co., Yellow Springs, Ohio.

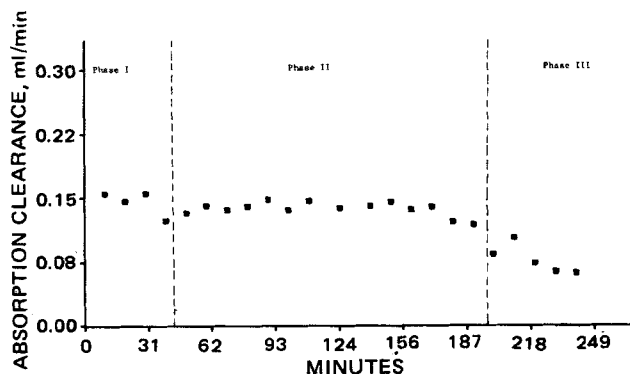


Figure 1—Relationship between the intestinal absorption clearance (Cl_A) and time for iopanoic acid to perfuse at a rate of $9.9 \mu\text{l}/\text{sec}$. The broken vertical lines delineate the three distinct phases within a particular study. Phase I represents an equilibration phase, Phase II is the phase of uniform clearance from which all comparisons are made, and Phase III is indicative of a physiological deterioration of the animal under prolonged anesthesia.

every 15 min for $3.1 \mu\text{l}/\text{sec}$ to ensure adequate volume collection for accuracy in the assay and in volume determination. Eight-minute intervals were used for sample collection at the flow rate of $20.5 \mu\text{l}/\text{sec}$ so as not to exceed the capacity of the collecting cylinders. Sample collection intervals of every 10 min were used for the other flow rates.

The volume at the end of each time interval was recorded, and the sample was mixed on a vortex mixer⁸ to ensure a homogeneous solution. A 2-ml aliquot then was placed in a 2.5-ml polystyrene vial⁹ and assayed for total iodine content by fluorescence excitation analysis (17). A standard curve was constructed by plotting the ratio ($NK\alpha/NC$) against known concentrations of iodine, prepared by dissolving appropriate amounts of sodium iodide¹⁰ in demineralized, double-distilled water to yield concentrations of 0.0, 0.25, 0.5, 1.0, 1.5, and $5.0 \mu\text{M}/\text{ml}$.

Standard curves were constructed routinely to verify the reliability of the assay. At no point was the correlation coefficient (r) less than 0.999. During the analysis of a set of samples from one experiment, standard samples were run periodically as a check for deviation in the standard curve. Most checks were within $\pm 2\%$. A deviation of 4% or greater was considered unacceptable, and a new standard curve was constructed. In such cases, the analysis was repeated starting from the first sample assayed using the previous standard curve.

At the end of the experiment, the animal was sacrificed and the intestinal segment was placed in an aluminum dish and oven dried at 110° for 48 hr. The dried intestine was weighed¹¹ accurately, and all clearance values were normalized to 100 mg of dry weight. The relationship between clearance and the dry intestinal weight was linear.

Absorption clearance (Cl_A) for each collection period was calculated using:

$$Cl_A = \left[\frac{C_{in} - C_{out}}{C_{in}} \right] \dot{V} \quad (\text{Eq. 1})$$

where \dot{V} is the measured perfusion flow for that collection period, C_{in} is the iopanoic acid concentration in buffer entering the gut segment, and C_{out} is the iopanoic acid concentration collected leaving the gut segment during the collection period.

RESULTS AND DISCUSSION

Iopanoic acid is a poorly absorbed cholecystographic agent. Its poor absorption has been implicated as the cause of some failures encountered during an initial examination since, upon repeat administration or doubling of the dose, 30% of those subjects with initial inadequate visualization showed excellent visualization (18–20). Therefore, nonvisualization must be confirmed by repeat examination or upon doubling of the dose at a future date before disease or obstruction can be considered a viable diagnosis.

Since absorption of iopanoic acid must be maximized to produce a

⁸ Bronwill, VWR Scientific, Brisbane, Calif.

⁹ Sherwood Medical Industries, St. Louis, Mo.

¹⁰ Mallinckrodt.

¹¹ Mettler H542 balance.

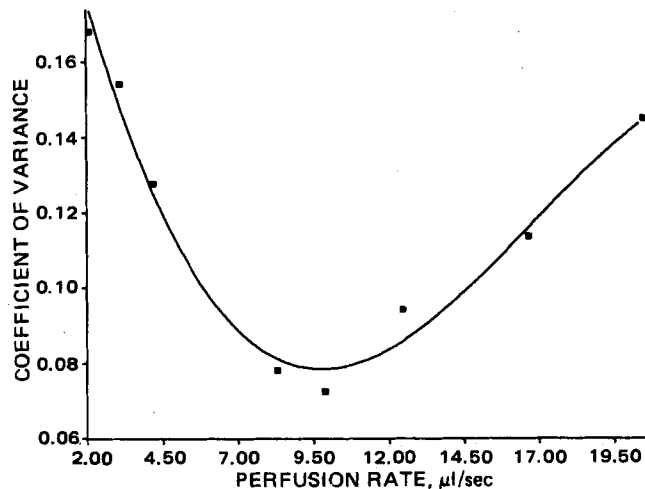


Figure 2—NONLIN computer fit for the third-order polynomial function relating the mean coefficient of variance in the absorption clearance and the intestinal perfusion rate.

desired effect, it was selected as a model compound to suggest a method of decreasing variability in the data collected, thereby giving more credence to the results of comparative treatments made to influence drug absorption and to delineate absorption mechanisms. Iopanoic acid also provides a quick, sensitive, and uncomplicated assay with essentially no manipulation involved.

The absorption clearance was measured and plotted as a function of time. A representative absorption clearance–time course is shown in Fig. 1. These clearance profiles have three distinct phases or sections. Phase I, lasting about 60–70 min, generally exhibited an apparent decrease in clearance with time; this result could be due to equilibration of water transport and failure to flush out totally the residual wash solution remaining within the segment at the start of the perfusion. Schanker *et al.* (6) reported a similar phenomenon during the initial phase of their absorption experiments. Podesta and Mettrick (21) also allowed a 20-min equilibration period in their perfusion experiments.

Phase II, characterized by relatively uniform clearance values from 40 to 180 min (and in some cases 240 min), was followed by a third phase of clearance. Phase III was attributed to a deterioration in the physiological condition of the rat under prolonged anesthesia. In separate studies, it was determined that back-diffusion of iopanoic acid from the blood to the lumen and its binding to the gut mucosa did not occur.

The scatter or variability of the data in Phase II of the clearance–time profiles appeared to be flow rate dependent. High scatter seemed to be associated with the fast and slow flow rates; low scatter was associated with intermediate flow rates. To discern the actual relationship, the mean coefficient of variance at each flow rate was calculated and plotted as a function of the flow rate (Fig. 2). The resultant plot resembled a parabolic function. The data were fitted subsequently to a series of polynomial functions as well as hyperbolic, logarithmic, exponential, and root functions. The equation giving the best fit and minimum sum of squares is:

$$Y = (-5.19 \times 10^{-5})x^3 + (2.65 \times 10^{-3})x^2 - (3.7 \times 10^{-2})x + 0.24 \quad (\text{Eq. 2})$$

where x is the flow rate (microliters per second) and Y is the coefficient of variance.

Solving the quadratic differential yielded a root of 9.89 for the minimum value. Six rat studies were conducted at the calculated optimal flow rate ($9.9 \mu\text{l}/\text{sec}$), predicted to provide the minimum coefficient of variance for the absorption clearance. These results gave the predicted minimum coefficient of variance (Table I). The results of the least-squares nonlinear regression analysis by Marquardt's gradient–expansion method (22) are given in Table II. The data obtained from the flow rate experiment performed at $9.9 \mu\text{l}/\text{sec}$ ($0.594 \text{ ml}/\text{min}$) were added to the results of the previous studies and again fitted to a series of polynomial functions. The final equation from the least-squares fit is given by Eq. 3 and was verified by successfully fitting the data using NONLIN (23):

$$Y = (-5.52 \times 10^{-5})x^3 + (2.784 \times 10^{-3})x^2 - (3.87 \times 10^{-2})x + 0.243 \quad (\text{Eq. 3})$$

Table I—Mean Coefficient of Variance and Standard Deviation of Absorption Clearance at Different Perfusion Rates

Perfusion Rate, $\mu\text{l}/\text{sec}$	n	Mean Coefficient of Variance	Standard Deviation between Experiments
2.1	4	0.1682	0.0339
3.1	8	0.1541	0.0568
4.2	5	0.1278	0.0394
8.3	5	0.0781	0.0182
9.9	6	0.0754	0.0164
12.5	6	0.0942	0.0252
16.7	7	0.1137	0.0355
20.5	7	0.1450	0.0170

The dependence of the coefficient of variance on flow seems to follow this polynomial relationship. From this relationship, the flow at which the coefficient of variance was minimized could be calculated. Thus, the optimal flow rate, which minimized the variability in the data, was determined to be $9.9 \mu\text{l}/\text{sec}$ ($0.594 \text{ ml}/\text{min}$).

The magnitude of the mean absorption clearance within the uniform phase (Phase II) was also dependent on the flow rate (Fig. 3) as noted previously (24). The higher flow rates produced higher absorption clearance values, which will be discussed.

An analysis for determining significant differences between the coefficients of variance at each flow rate was performed. Since multiple comparisons were to be made, the linear contrast method, Fisher's protected least significant difference (25), was selected over multiple t tests to minimize the overall error rate. The overall error rate to t test comparisons is given by:

$$\text{overall error rate} = 1 - (1 - \alpha)^c \quad (\text{Eq. 4})$$

The term α is a value between 0 and 1 and denotes the probability of incurring type I errors (falsely rejecting the null hypothesis), and c is the number of comparisons made. Thus, the error rate increases with an increasing number of comparisons. Therefore, if multiple comparisons between the eight flow rates are made, the probability of falsely rejecting the null hypothesis (the means of the coefficients of variance at two flow rates are equal) on at least one t test becomes quite large. The calculated F ratio (6.36) is much larger than the tabulated value (3.3) at $\alpha = 0.01$. The least significant difference (LSD) for each comparison was calculated by:

$$LSD = t_{\alpha/2} \sqrt{S^2w \left(\frac{1}{N_i} + \frac{1}{N_j} \right)} \quad (\text{Eq. 5})$$

where $t_{\alpha/2}$ denotes the tabulated critical t value for a two-tailed test, N_i and N_j are the respective sample sizes, and S^2w is the mean square within samples obtained from a one-way analysis of variance.

The results of the LSD were: (a) 9.9 and $8.3 \mu\text{l}/\text{sec}$ were significantly less than $2.1, 3.1, 4.2,$ and $20.5 \mu\text{l}/\text{sec}$ at $p < 0.01$ and significantly less than $16.7 \mu\text{l}/\text{sec}$ at $p < 0.05$; (b) $12.5 \mu\text{l}/\text{sec}$ was significantly less than $2.1, 3.1,$ and $20.5 \mu\text{l}/\text{sec}$ at $p < 0.005$; and (c) $16.7 \mu\text{l}/\text{sec}$ was significantly less than $2.1 \mu\text{l}/\text{sec}$ at $p < 0.005$ and significantly less than $3.1 \mu\text{l}/\text{sec}$ at $p < 0.05$.

Table II—Nonlinear Least-Squares Regression Analysis^a for the Mean Coefficient of Variance versus Flow Rate Curve

X^b	$Y(\text{obs})^c$	$Y(\text{calc})^c$	Deviation
2.1	0.1682	0.1735	-0.0053
3.1	0.1541	0.1482	0.0060
4.2	0.1278	0.1255	0.0023
8.3	0.0781	0.0822	-0.0041
9.9	0.0754	0.0794	-0.0040
12.5	0.0942	0.0868	0.0074
16.7	0.1137	0.1165	-0.0028
20.5	0.1450	0.1445	0.0048

weighting = 1
 variance = 411.42×10^{-7}
 standard deviation = 0.0064
 correlation coefficient = 0.9904
 r -square = 0.9804
 sum of squares of error = 164.57×10^{-6}
 percent error reduction = 99.8

^a By Marquardt's gradient-expansion method (22). ^b Flow rate, microliters per second. ^c Coefficient of variance.

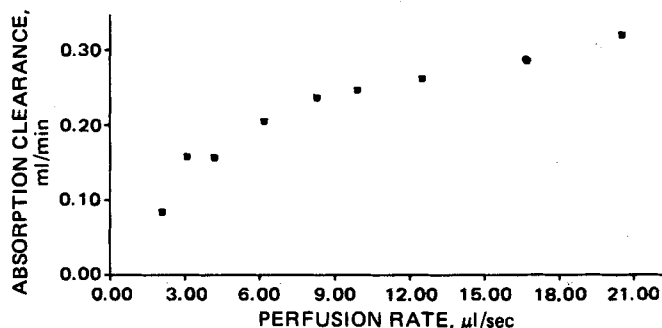


Figure 3—Relationship between the mean absorption clearance and the intestinal perfusion rate.

No significant difference was observed among $8.3, 9.9,$ and $12.5 \mu\text{l}/\text{sec}$ ($p > 0.1$). The coefficient of variance for $16.7 \mu\text{l}/\text{sec}$ did not differ significantly from the coefficient of variance for $12.5 \mu\text{l}/\text{sec}$ but was significantly different from 8.3 and $9.9 \mu\text{l}/\text{sec}$ at $p < 0.01$. Because of this latter result, the optimal flow rate, which could aid in the experimental design and improve the results of subsequent absorption studies, should be between 8 and $10 \mu\text{l}/\text{sec}$ rather than between 8 and $13 \mu\text{l}/\text{sec}$.

In vivo work by Hollander and coworkers (2, 3), who used flow rates of $0.5, 1.0, 2.5, 5.0,$ and $10.0 \text{ ml}/\text{min}$ to study their effect on vitamin A_1 and vitamin K_1 absorption, tends to support the present work. Use of their data to calculate a coefficient of variance reveals that the minimum coefficient of variance occurred at $0.5 \text{ ml}/\text{min}$ ($8.3 \mu\text{l}/\text{sec}$). The maximum variability occurred between 1.0 and $2.5 \text{ ml}/\text{min}$. Koezumi *et al.* (26), using flow rates of $2.5, 5.0, 6.5,$ and $10.0 \text{ ml}/\text{min}$ to study the absorption rate of unionized sulfamerazine, reported data that, by our calculations, revealed low coefficient of variance values. Rates above $1.5 \text{ ml}/\text{min}$ become, in a sense, nonphysiological, and the decrease in or the low coefficient of variance values become an artifact of the high perfusion rate. Such high rates do not allow for subtle intraluminal influences normally affecting drug transport across the mucosal barrier. These large values for the absorption rate increase the denominator in the calculation of the coefficient of variance, thereby making it small and reflecting perhaps the efficiency of the pump delivering the perfusate.

The convective diffusion model of Nelson and Shah (27-29) was selected to describe the effects of flow rates on the absorption clearance. Originally used to describe the drug dissolution rate (27, 28) and later membrane transport (29), the model gives the equation for the dissolution rate (R) across the surface of a rectangle of length L and width b as:

$$R = 0.808D^{2/3}C_0\alpha^{1/3}bL^{2/3} \quad (\text{Eq. 6})$$

where D is the diffusivity, C_0 is the solubility (usually given as the initial concentration in the donor phase), and α represents the shear rate adjacent to the planes for flow between two parallel planes and is defined as:

$$\alpha = \frac{6Q}{H^2W} \quad (\text{Eq. 7})$$

where Q is the volumetric flow rate and H and W are the height and width of the channel in the diffusion cell, respectively. If a cylinder is considered to be a good approximation of the intestinal membrane surface, the corresponding equation for the absorption rate (R) is:

$$R = 0.808D^{2/3}C_0\alpha^{1/3}2\pi rL^{2/3} \quad (\text{Eq. 8})$$

The initial concentration in the perfusing solution (C_0) changes as a result of absorption. To account for absorption and the subsequent concentration gradient, the "logarithmic mean," $(C_0 - C_2)/\ln(C_0/C_2)$, was used as the best average for laminar flow through a solute-permeable tube (30). Dividing Eq. 8 by this logarithmic mean for the concentration results in the absorption clearance expression:

$$Cl_A = 0.808D^{2/3}\alpha^{1/3}2\pi rL^{2/3} \quad (\text{Eq. 9})$$

The shear rate (α), relating the linear velocity with the distance away from the surface over which the flow occurs (Eq. 7), is for flow between two planes; however, a similar expression can be derived for the shear rate through a cylinder. If it is assumed that the intestinal segment is long enough to avoid end effects, the velocity distribution for a liquid under steady laminar flow through the cylinder of length L and radius r is a parabolic function given by (31):

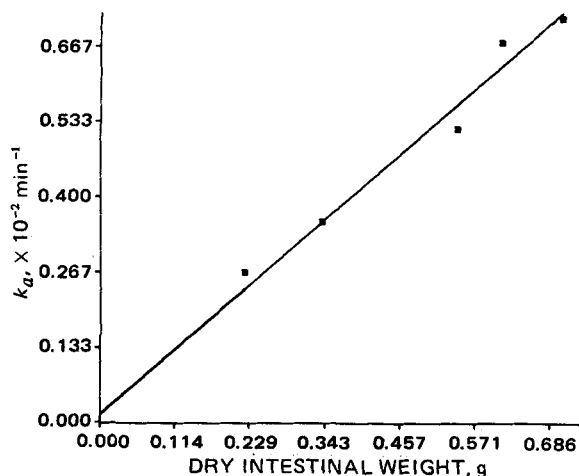


Figure 4—Linear relationship between the first-order absorption rate constant (k_a) and the dry intestinal weight. The correlation coefficient of the regression line is 0.9933 with a corresponding slope of 0.01 (g min^{-1}) $^{-1}$. The intercept of 0.0001 was not statistically different from zero ($p < 0.05$).

$$V_z = \frac{\Delta P r^2}{4\eta L} \left[1 - \left(\frac{r'}{r} \right)^2 \right] \quad (\text{Eq. 10})$$

where η is the viscosity that is the proportionality constant relating the shear rate and the shearing stress and ΔP is the pressure drop over the intestinal segment and represents the combined effect of static pressure and gravitational force. The volumetric flow rate (Q) is given by the well-known Hagen-Poiseuille law (31):

$$Q = \frac{\pi(\Delta P)r^4}{8\eta L} \quad (\text{Eq. 11})$$

Differentiating the velocity with respect to r' , the radial distance from the parabolic maximum velocity (center of the tube), results in an expression for the shear rate given by:

$$\alpha = \frac{dV_z}{dr'} = \left(\frac{-\Delta P}{2\eta L} \right) r' \quad (\text{Eq. 12})$$

Since the concern is with stress against the absorbing surface, this point of maximal stress occurs where r' equals the radius r . Solving Eq. 11 for ΔP and substituting into Eq. 12 give an expression relating the shear rate and the volumetric flow rate for laminar flow through a tube:

$$\alpha = \frac{4Q}{\pi r^3} \quad (\text{Eq. 13})$$

Winne (32) reported that the length and intraluminal radius of the perfused segment were not altered when the perfusion rate was varied from 0.1 to 0.5 ml/min. Lewis and Fordtran (15) showed that the intraluminal pressure did not change when the perfusion rate was raised

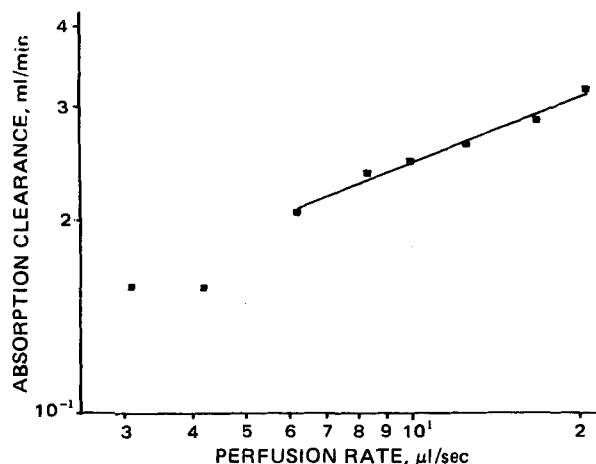


Figure 5—Log-log plot of the absorption clearance as a function of the intestinal perfusion rate in accord with the convective diffusion model.

from 1 to 10 ml/min. These reports indicate that the radius can be considered a constant over the range of rates used.

The linear relationship between Cl_A and the dry intestinal weight, previously mentioned, was also noted between the first-order absorption rate constant and the dry intestinal weight (Fig. 4). This figure suggests that, on normalization, the only variable becomes the flow rate. By combining constants, Eq. 9 reduces to a simplified format exemplified by:

$$Cl_A = NQ^{1/3} \quad (\text{Eq. 14})$$

where N is the constant product of all other terms.

In accord with Eq. 14, a plot of $\log Cl_A$ versus $\log Q$ should result theoretically in a straight line with a theoretical slope of 0.33. The experimental results are plotted in Fig. 5. The resulting slope is 0.339 with a correlation coefficient of 0.992 for rates between 6.2 and 20.5 $\mu\text{l}/\text{sec}$. This experimental slope value indicates excellent correlation with the theoretical value for the convective diffusion model hypothesis. Even when the rates of 3.1 and 4.2 $\mu\text{l}/\text{sec}$ are included in the statistical analysis, the resultant least-squares slope of 0.388 still is in reasonable accord with the model. The slight deviation from theory on addition of the lower flow rates may be the result of longer resident times within the segment, possibly reflecting more complex absorption phenomena resulting from the invaginations between villi not accounted for in the simple cylinder shape assumption.

The literature abounds with discussions on the aqueous diffusion layer adjacent to the mucosal wall and its influence on the absorptive process. The convective diffusion model not only accounts for simple diffusion through this layer but allows for fluid flow and convection, which has been very useful in modeling the absorptive process for iopanoic acid in these studies. The increase in clearance with increasing flow rate probably was due to increased shear adjacent to the membrane, which increased the concentration gradient normal to it, since the surface area does not seem to be greatly affected (32) until rates above 10 ml/min are used (15).

In summary, the present studies suggest that there is a singular region in which the flow rate in an *in situ* perfusion system maximizes the reliability of the data collected. Minimizing the coefficient of variance lends more credence to observed data, providing more reliable parameters for comparative studies.

Knowing the optimal flow rate at which to perform perfusion experiments *in vivo* will permit more precise comparisons of the effects of modifying agents (*e.g.*, ions, nutrients, bile salts, and other drugs) on mucosal transport of a given solute.

REFERENCES

- (1) S. Kitazawa, M. Ishizir, and E. Arakawa, *Chem. Pharm. Bull.*, **24**, 3169 (1976).
- (2) D. Hollander, E. Rim, and K. S. Muralidhara, *Am. J. Physiol.*, **232**, E69 (1977).
- (3) D. Hollander and K. S. Muralidhara, *ibid.*, **232**, E471 (1977).
- (4) C. A. M. Hogben, D. J. Tocco, B. B. Brodie, and L. S. Schanker, *J. Pharmacol. Exp. Ther.*, **125**, 275 (1959).
- (5) C. A. M. Hogben, L. S. Schanker, D. J. Tocco, and B. B. Brodie, *ibid.*, **120**, 540 (1957).
- (6) L. S. Schanker, D. J. Tocco, B. B. Brodie, and C. A. M. Hogben, *ibid.*, **123**, 81 (1958).
- (7) L. S. Schanker, P. A. Shore, B. B. Brodie, and C. A. M. Hogben, *ibid.*, **120**, 528 (1957).
- (8) P. A. Shore, B. B. Brodie, and C. A. M. Hogben, *ibid.*, **119**, 361 (1957).
- (9) S. Feldman and M. Gibaldi, *Proc. Soc. Exp. Biol. Med.*, **132**, 1031 (1969).
- (10) K. Kakemi, H. Sezaki, R. Konishi, T. Kimura, and M. Murakami, *Chem. Pharm. Bull.*, **18**, 275 (1970).
- (11) T. S. Gaginella, P. Bass, J. H. Perrin, and J. J. Vallner, *J. Pharm. Sci.*, **62**, 1121 (1973).
- (12) C. F. Cramer and T. A. Haqq, *Can. J. Biochem. Physiol.*, **41**, 127 (1963).
- (13) A. M. Dawson and H. B. McMichael, *Proc. Phys. Soc.*, **2-3**, 13P (1968).
- (14) C. D. Holdsworth and A. M. Dawson, *Clin. Sci.*, **27**, 371 (1964).
- (15) L. D. Lewis and J. S. Fordtran, *Gastroenterology*, **68**, 1509 (1975).
- (16) J. T. Doluisio, G. H. Tan, N. F. Billups, and L. Diamond, *J. Pharm. Sci.*, **58**, 1200 (1969).
- (17) J. L. Kaufman, J. Nelson, and D. Price, *IEEE Trans. Nucl. Sci.*

NS, 20, 402 (1973).

(18) R. M. Taketa, R. N. Berk, J. H. Lang, E. C. Lasser, and C. R. Dunn, *Am. J. Roentgenol.*, 114, 767 (1972).

(19) L. E. Goldberger, R. N. Berk, J. H. Lang, and P. M. Loeb, *Invest. Radiol.*, 9, 16 (1974).

(20) H. D. Rosebaum, *Am. J. Roentgenol.*, 82, 1011 (1959).

(21) R. B. Podesta and D. F. Metrick, *Am. J. Physiol.*, 232, E62 (1977).

(22) P. R. Bevington, "Data Reduction and Error Analysis for the Physical Sciences," McGraw-Hill, New York, N.Y., 1969, p. 235.

(23) C. M. Metzler, "NONLIN, A Computer Program for Parameter Estimation in Non-Linear Situations," Upjohn Co., Kalamazoo, Mich., 1969.

(24) I. Komiya, J. Y. Park, A. Kamani, N. F. H. Ho, and W. I. Higuchi, "Abstracts," vol. 9 (2), APhA Academy of Pharmaceutical Sciences, Washington, D.C., 1979, p. 84.

(25) L. Ott, "An Introduction to Statistical Methods and Data Analysis," Wadsworth Publishing, Belmont, Calif., 1977, p. 384.

(26) T. Koezumi, T. Arita, and K. Kakemi, *Chem. Pharm. Bull.*, 12, 421 (1964).

(27) K. G. Nelson and A. C. Shah, *J. Pharm. Sci.*, 64, 610 (1975).

(28) A. C. Shah and K. G. Nelson, *ibid.*, 64, 1518 (1975).

(29) K. G. Nelson and A. C. Shah, *ibid.*, 66, 137 (1977).

(30) D. Winne and I. Markgraf, *Naunyn-Schmiedeberg Arch. Pharmacol.*, 309, 271 (1979).

(31) R. B. Bird, W. E. Stewart, and E. N. Lightfoot, "Transport Phenomena," Wiley, New York, N.Y., 1960, p. 42.

(32) D. Winne, *Naunyn-Schmiedeberg Arch. Pharmacol.*, 307, 265 (1979).

ACKNOWLEDGMENTS

Presented in part at the Basic Pharmaceutics Section, APhA Academy of Pharmaceutical Sciences, Washington meeting, April 1980.

The authors thank Ms. Sue Sheffield for her skilled secretarial assistance.

Mixing of Pharmaceutical Solids II: Evaluation of Multicomponent Mixing of Cohesive Powders in Cylindrical Shear Mixer

Z. T. CHOWHAN *, E. E. LINN, and LI-HUA CHI

Received November 1, 1979, from Syntex Research, Palo Alto, CA 94304.

Accepted for publication August 14, 1980.

Abstract □ The mixing of three organic carboxylic acids with micronized lactose, all cohesive in nature, was studied using a cylindrical shear mixer. Three mixing indexes (s/σ_A , s/σ_R , and the Ashton-Valentin mixing index) were used to evaluate mixing of the three drugs with lactose. The results suggested that maximum homogeneity was reached after 45 min of mixing. However, different mixing indexes showed different sensitivity to homogeneity of the individual components. The mixing index s/σ_A , which is based on setting standard specifications, appears to provide a better evaluation of homogeneity of individual components compared to the mixing indexes based on complete random mixing theory. The latter did not approach unity for any drug component used in this study. These results suggested that mixing of cohesive powders is a complex process and cannot be explained fully by simple theory based on complete random mixing.

Keyphrases □ Mixing—of multicomponent cohesive powders, evaluation of homogeneity using three mixing indexes based on statistical analysis □ Powders—multicomponent mixing of cohesive powders, evaluation of homogeneity using three mixing indexes based on statistical analysis □ Carboxylic acids—cohesive powders mixed with lactose for homogeneity evaluation, evaluation of three mixing indexes based on statistical analysis □ Dosage forms, design—multicomponent mixing of cohesive powders to determine homogeneity of individual components, three mixing indexes evaluated

The mixing of a cohesive drug with cohesive, noncohesive, and free-flowing excipients was studied previously (1) using two types of mixers, cylindrical shear and V-shaped tumbling. Most mixing studies use binary systems, and mixing indexes based on statistical analysis are used to evaluate homogeneity. However, many practical situations in dosage form design require mixing several powders. Although most multicomponent mixing has been studied theoretically (2-6), one practical multicomponent system used 10% phenobarbital, 1% secobarbital, 1% butobarbital, and 88% lactose (7-9).

The multicomponent mixing of cohesive powders is one of the most difficult and complex powder mixing systems. None of the reported mixing studies have dealt with this powder mixing system.

This paper reports the mixing of cohesive powders of three organic carboxylic acids and an excipient in a cylindrical shear mixer. The results were evaluated by the mixing indexes based on complete random mixing and on standard specifications described previously (10, 11).

EXPERIMENTAL

Materials—Three organic carboxylic acids, 7-methylsulfinyl-2-xanthone carboxylic acid (I), 7-methylthio-2-xanthone carboxylic acid (II), and 5-isopropoxy-7-methylthio-2-xanthone carboxylic acid (III), and mestranol were at least 99% pure¹. USP grade lactose² was micronized³. Component I was micronized, and II and III were used as received. Methanol⁴ was spectra grade, and polysorbate 80⁵ was USP grade. All other chemicals were analytical grade unless specified otherwise.

Physical Properties—The particle-size distributions of I-III were determined⁶ by electronic counting. The vehicle was a saturated solution of the compound in 0.6% HCl containing 0.018% polysorbate 80. The filtered vehicle was used to disperse the drug powder.

The particle-size distribution of the micronized lactose was determined⁷ by automatic sedimentation, using photoextinction to measure the apparent projected area at decreasing sedimentation depths with increasing time.

The densities of the organic carboxylic acids were determined by the density matching method of Oster and Yamamoto (12). Mixtures of

¹ Institute of Organic Chemistry, Syntex Research, Palo Alto, CA 94304.

² Lactose regular, Foremost Food Co., San Francisco, CA 94104.

³ Jet Pulverizer Co., Palmyra, N.J.

⁴ Mallinckrodt Chemical Works, St. Louis, MO 63160.

⁵ ICI America, Atlas Chemical Division, Wilmington, Del.

⁶ Coulter counter model TA, Coulter Electronics, Hialeah, FL 33010.

⁷ Sedigraph-L Micromeritics Instrument Corp., Norcross, Ga.